# Broken mirror symmetry in excitonic response of reconstructed domains in twisted MoSe₂/MoSe₂ bilayers

Jiho Sung[1,2], You Zhou [1,2], Giovanni Scuri [2], Viktor Zólyomi[3,4], Trond I. Andersen[2], Hyobin Yoo[2,5], Dominik S. Wild [2], Andrew Y. Joe[2], Ryan J. Gelly[2], Hoseok Heo[1,2], Samuel J. Magorrian [3], Damien Bérubé[6], Andrés M. Mier Valdivia[7], Takashi Taniguchi[8], Kenji Watanabe [8], Mikhail D. Lukin[2], Philip Kim [2,7], Vladimir I. Fal'ko [3,9] ✉ and Hongkun Park [1,2] ✉

[1]Department of Chemistry and Chemical Biology, Harvard University, Cambridge, MA, USA. [2]Department of Physics, Harvard University, Cambridge, MA, USA. [3]National Graphene Institute, University of Manchester, Manchester, UK. [4]Hartree Centre, STFC Daresbury Laboratory, Daresbury, UK. [5]Department of Physics, Sogang University, Seoul, Republic of Korea. [6]Department of Physics, California Institute of Technology, Pasadena, CA, USA. [7]John A. Paulson School of Engineering and Applied Sciences, Harvard University, Cambridge, MA, USA. [8]National Institute for Materials Science, Tsukuba, Japan. [9]Henry Royce Institute for Advanced Materials, University of Manchester, Manchester, UK. ✉e-mail: Vladimir.Falko@manchester.ac.uk; Hongkun_Park@harvard.edu

**Supplementary Information for "Broken mirror symmtery in excitonic response of reconstructed domains in twisted MoSe₂/MoSe₂ bilayers"**

Jiho Sung[1,2], You Zhou[1,2], Giovanni Scuri[2], Viktor Zólyomi[3,4], Trond I. Andersen[2], Hyobin Yoo[2,5], Dominik S. Wild[2], Andrew Y. Joe[2], Ryan J. Gelly[2], Hoseok Heo[1,2], Samuel J. Magorrian[3], Damien Bérubé[6], Andrés M. Mier Valdivia[7], Takashi Taniguchi[8], Kenji Watanabe[8], Mikhail D. Lukin[2], Philip Kim[2,7], Vladimir I. Fal'ko[3,9†] & Hongkun Park[1,2†]

[1]Department of Chemistry and Chemical Biology and [2]Department of Physics, Harvard University, Cambridge, MA 02138, USA

[3]National Graphene Institute, University of Manchester. Booth St. E., Manchester M13 9PL, United Kingdom

[4]Hartree Centre, STFC Daresbury Laboratory, Daresbury, WA4 4AD, United Kingdom

[5]Department of Physics, Sogang University, Seoul, 04107, Republic of Korea

[6]Department of Physics, California Institute of Technology, Pasadena, CA, 91125, USA

[7]John A. Paulson School of Engineering and Applied Sciences, Harvard University, Cambridge, MA 02138, USA

[8]National Institute for Materials Science, 1-1 Namiki, Tsukuba 305-0044, Japan

[9]Henry Royce Institute for Advanced Materials, University of Manchester, Manchester M13 9PL, United Kingdom

†To whom correspondence should be addressed: Hongkun_Park@harvard.edu and Vladimir.Falko@manchester.ac.uk
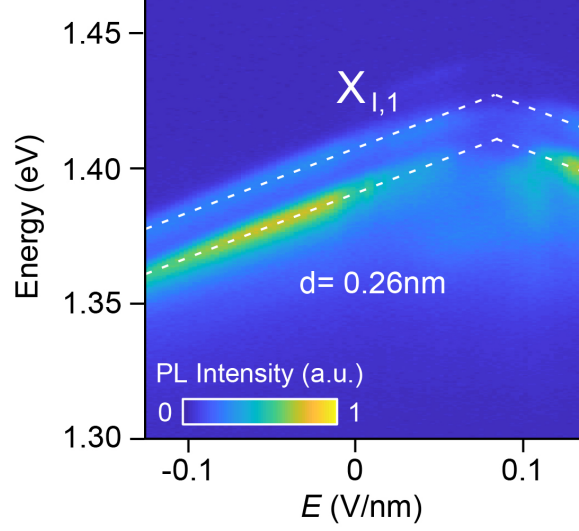
**Supplementary Figure 1. Electric dipole moment of the X$_{I,1}$-interlayer exciton and possible origin of the multiple peaks.** PL spectra of the X$_{I,1}$ peaks as a function of the electric field at spot 2 obtained from **D2**. The top and bottom g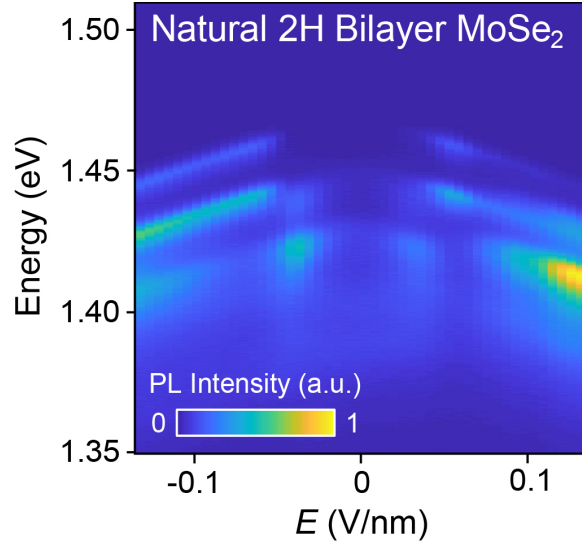ate voltages are swept together with a voltage ratio, -α (α = 39/42, the bottom hBN thickness over the top hBN thickness, $V_{BG}$ = -α × $V_{TG}$) in order to keep **D2** close to zero doping concentration, while applying an electric field. From the slope of the linear Stark shift, we obtain the magnitude of the interlayer exciton dipole moment using the formula $\Delta E = -edE_z$, where $E$ is the energy of emission, $e$ is the electric charge, $d$ is the distance between an electron and a hole, and $E_z$ is the applied out-of-plane electric field. The applied out-of-plane electric field was calculated with the formula, $E_z = (C_{Bottom,hBN}V_{BG} - C_{Top,hBN}V_{TG})/2\varepsilon_{biMoSe2}$, where $C_{Bottom,hBN} = \varepsilon_{hBN}/d_{Bottom,hBN}$ and $C_{Top,hBN} = \varepsilon_{hBN}/d_{Top,hBN}$ are the geometric capacitance of the bottom and top hBN, $V_{BG}$ and $V_{TG}$ are the applied bottom and top gate voltages and $\varepsilon_{biMoSe2}$ is the dielectric constant of bilayer MoSe$_2$. We use $\varepsilon_{hBN}$ = 3.5 and $\varepsilon_{biMoSe2}$ = 7.9, which were reported in the literature [S1].

We observe that the energy separation of these low energy peaks is independent of out-of-plane electric field in twisted bilayer MoSe$_2$, suggesting that the multiple peaks are from the same Γ−K transition. Based on their splitting of 18-20 meV, one possibility is that the peaks are phonon replicas [S2]. The phonon modes available for scattering of the electron from the K point to the Γ point (zone-edge phonon modes, assuming quasi-momentum conservation) have energies of 16.6 and 19.9 meV for the transverse acoustic (TA) and longitudinal acoustic (LA) phonons, and 35.5, 37,4 and 25.6 meV for the transverse optical (TO), longitudinal optical (LO) and A$_1$ optical

phonons [S3]. These observations suggest that the first peak could be the TA and LA acoustic phonon-assisted optical transition, and the second peak could be the TO, LO and $A_1$ optical phonon-assisted optical transition. Finally, the third peak could be from sidebands of higher order processes assisted by combination of multiple phonons, including TA and LA acoustic phonons and zone-centre optical phonons (36.1, 36.6 and 30.3 meV for TO, LO and $A_1$) [S4]. Nevertheless, more experiments and theoretical studies are required to fully understand which of the phonon modes are responsible for the phonon-assisted photoluminescence from the $\Gamma$−K transition in twisted bilayer $MoSe_2$.

**Supplementary Figure 2. Electric-field dependent PL spectra in a natural bilayer MoSe₂ device, D3 at 4K.** The top and bottom gate voltages are swept together with a voltage ratio, -1 (the thicknesses of the top and bottom hBN are both 48 nm) in order to keep **D3** close to zero doping concentration. We observe three low energy PL peaks, separated by ~18 meV, similar to the multiple-peak structures near 1.4 eV in the t-MoSe₂/MoSe₂ bilayers. The energy separation between these low energy PL peaks does not change as a function of the electric field as well.
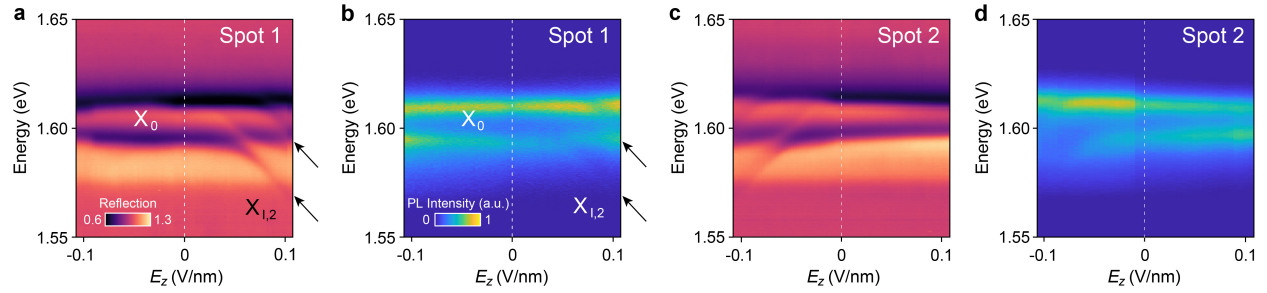
**Supplementary Figure 3. Electric field dependent reflectance and PL spectra of the $X_0$ and $X_{I,2}$ peaks obtained from D2 at 4K.** We measure the PL spectra with the same gate operation scheme as the reflectance measurements in Fig. 3 in the main text at **(b)** spot 1 and **(d)** spot 2. Two strong PL peaks at 1.594 eV and 1.610 eV are observed, whose energies do not change as a function of the out-of-plane electric field. The PL spectra match the reflectance spectra at **(a)** spot 1 and **(c)** spot 2: near $|E_z| = 0.07$ V/nm we observe an avoided crossing of the lower $X_0$ peak and the $X_{I,2}$ peak.
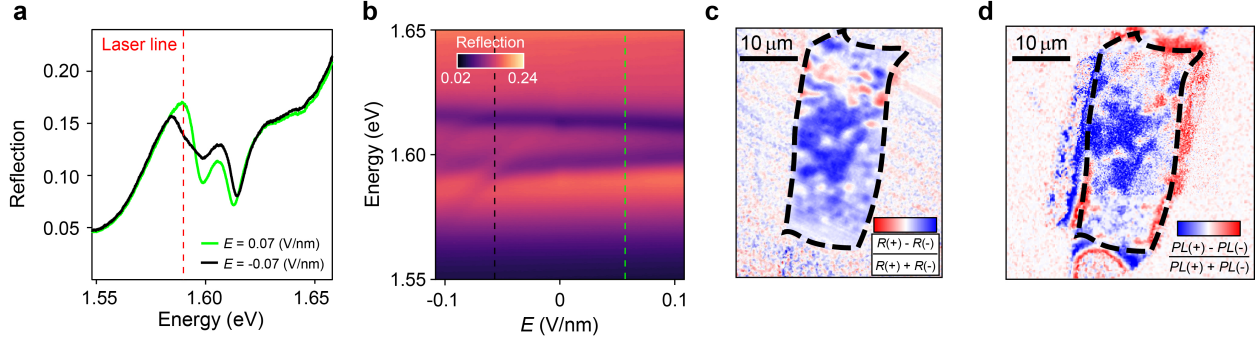
**Supplementary Figure 4. Spatial image of the avoided crossing features at 4K (a)** Cross sections of the reflectance spectra at spot 2 in **D2** along the green (at $E_z = 0.07$ V/nm) and black (at $E_z = -0.07$ V/nm) dashed lines in **(b)**. To obtain absolute reflectance, we normalize the reflected intensity using the measured reflectance of the metal electrodes. We spatially image the avoided crossing features by mapping out the reflection at two opposite electric fields ($\pm 0.07$ V/nm), using a continuous wave laser centred at 1.59 eV (red line in **(a)**). **(c)** A map of the ratio $\xi = \frac{R_+ - R_-}{R_+ + R_-}$, calculated from the reflection data is shown ($R_\pm$ is the reflected intensity at $E_z = \pm 0.07$ V/nm). The spatial dependence of the avoided crossing features matches well with the interlayer dipole orientation map in **(d)**, indicating that these features have a common physical origin. We flipped the colour bar in (c) to match the colour scheme with the map of $\eta = \frac{PL_+ - PL_-}{PL_+ + PL_-}$: this is because the reflected intensity is smaller when there is an avoided crossing.
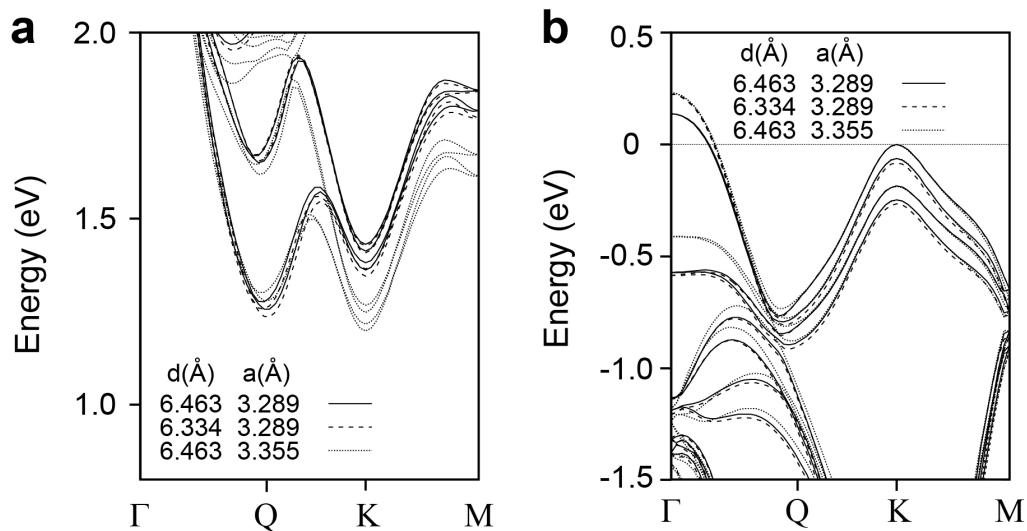
**Supplementary Figure 5. Electronic band structure of the AB-stacked MoSe$_2$/MoSe$_2$ bilayer from the DFT calculation.** DFT calculated **(a)** conduction and **(b)** valence bands of the AB-stacked MoSe$_2$/MoSe$_2$ bilayer, with the energies counted from the local valence band maximum (VBM) at K point. Interlayer distance, $d$ and lattice constant, $a$ are set to different values for which the band dispersions are plotted with solid, dashed and dotted lines.
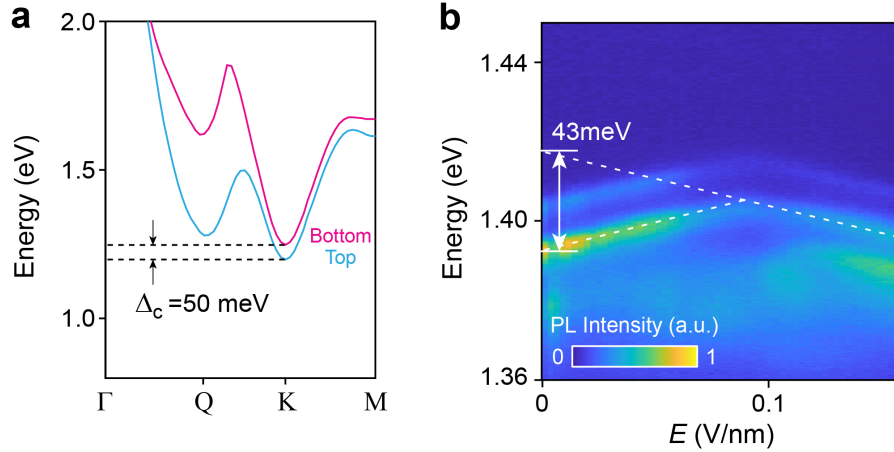
**Supplementary Figure 6. Estimating the splitting between the top and bottom layer K valley conduction band minimum (CBM). (a)** The calculated conduction band of AB-stacked MoSe$_2$/MoSe$_2$ using DFT. The band where electrons are more localized in the top (bottom) MoSe$_2$ layer is shown in cyan (magenta) colour. At the K point, there is a splitting ($\Delta_c$) between the top and bottom MoSe$_2$ layer. At $E_z$=0, electrons in the K point, which is the CBM, are localized in the top layer. A positive electric field decreases $\Delta_c$ by making the electrons in the bottom layer more energetically favorable. Spin flipped upper conduction bands are not plotted for the clarity. The calculated value of $\Delta_c$ is 50 meV. **(b)** We can estimate $\Delta_c$ at zero electric field by extrapolating the line with a negative slope to zero field in the PL spectrum. The extracted value is ~43 meV, in good agreement with the calculated value of 50 meV. By comparison, the calculated conduction band splitting at the Q point is ~400 meV. This splitting would require a field larger than 3.3 V/nm to switch the preferred dipole orientation of the $\Gamma$−Q interlayer excitons (based on the calculated dipole moment of Q valley electrons of ~0.06 (e·nm)). This electric field value is much larger than the field at which we observe the transition (0.09 V/nm), suggesting that the CBM is at the K point.
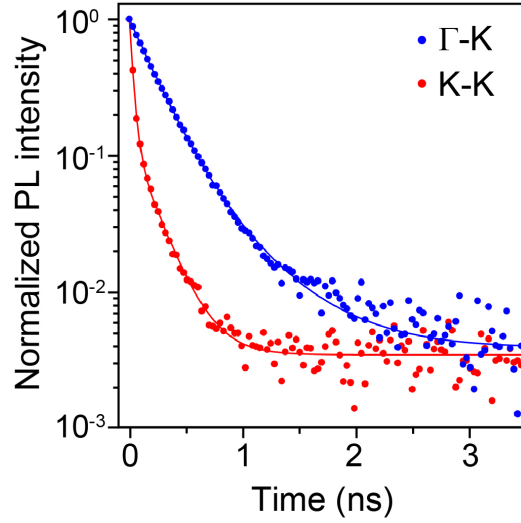
**Supplementary Figure 7. Time-resolved PL measurements for the $X_{I,1}$-interlayer excitons ($\Gamma-K$ transition: blue dots) and hybridized $X_0$-$X_{I,2}$ excitons (K-K transition: red dots).** To measure the lifetime of the hybridized $X_0$-$X_{I,2}$ excitons, we apply $E_z = \pm 0.07$ V/nm and collect only the emission from lower-energy intralayer excitons around 1.594 eV. Based on the bi-exponential fits with an offset (blue and red solid lines), the extracted fast and slow time scales are: $\tau_1$=0.21 ns and $\tau_2$=0.50 ns for the $X_{I,1}$-interlayer excitons and $\tau_1$=0.03 ns and $\tau_2$=0.19 ns for the hybridized $X_0$-$X_{I,2}$ excitons. We used average laser power of 2 $\mu$W to minimize nonlinear or nonequilibrium decay and maintain good signal to noise.

## References

[S1]    Laturia, A., Van de Put, M. L. & Vandenberghe, W. G. Dielectric properties of hexagonal boron nitride and transition metal dichalcogenides: from monolayer to bulk. *NPJ 2D Mater. and Appl.* **2**, 6 (2018).

[S2]    Wang, Z., Chiu, Y.-H., Honz, K., Mak, K. F. & Shan, J. Electrical tuning of interlayer exciton gases in WSe$_2$ bilayers. *Nano Lett.* **18**, 137-143 (2018).

[S3]    Jin, Z., Li, X., Mullen, J. T. & Kim, K. W. Intrinsic transport properties of electrons and holes in monolayer transition-metal dichalcogenides. *Phys. Rev. B* **90**, 045422 (2014).

[S4]    Dery, H. & Song, Y. Polarization analysis of excitons in monolayer and bilayer transition-metal dichalcogenides. *Phys. Rev. B* **92**, 125431 (2015).